



Theoretical Simulation of Thermal Deformations in Concrete Beams Reinforced with Two Overlapped FRP Bars in Cold Regions

Ali Zaidi

Professor, Structure Rehabilitation and Materials Laboratory (SREML), University of Laghouat, Laghouat, Algeria;
Associate Professor, Department of Civil and Building Engineering, University of Sherbrooke, Sherbrooke, QC., Canada
a.zaidi@lagh-univ.dz

Hizia Bellakehal

Structure Rehabilitation and Materials Laboratory (SREML), University of Laghouat, Laghouat, Algeria
h.bellakehal@lagh-univ.dz

Radhouane Masmoudi

Department of Civil and Building Engineering, University of Sherbrooke, Sherbrooke, QC., Canada
Radhouane.Masmoudi@USherbrooke.ca

Oumelkhir Terbagou

Structure Rehabilitation and Materials Laboratory (SREML), University of Laghouat, Laghouat, Algeria
rimassrimass1995@gmail.com

Naima Nia

Structure Rehabilitation and Materials Laboratory (SREML), University of Laghouat, Laghouat, Algeria
sreml@lagh-univ.dz

Abstract

The thermal incompatibility in transverse direction between concrete and fiber reinforced polymer (FRP) bars may cause tensile circumferential cracks within concrete under low temperatures, and consequently, the failure of concrete cover. This paper presents a theoretical study to investigate the transverse thermal deformation of concrete beams reinforced with two overlapped FRP bars in cold regions where the climate temperature may drop to -40°C . Numerical and analytical models are developed to predict the transverse thermal strains at the FRP bar/concrete interface of the concrete cover zone and the bars interaction zone and also at the external surface of concrete cover for overlapped glass FRP (GFRP) bars reinforced concrete beams under low temperature variations, having a ratio of concrete cover thickness to FRP bar diameter varied from 1.0 to 3.2. Comparisons between the results predicted from non-linear finite element model and those obtained from the analytical model in terms of transverse thermal strains are presented.

Keywords: Low temperatures; Overlapped GFRP bars; Transverse deformations; Concrete cover; Cracking thermal loadings

1 Introduction

Various deteriorated reinforced concrete constructions (bridges and parking) due to the corrosion of steel bars need repairs. However, the repair cost of deficient structures can be estimated to billions of dollars. Numerous studies were carried out to substitute the steel by an anticorrosive material such as fibers reinforced polymer (FRP). This composite material is characterized by high immunity to corrosion, lightweight, high tensile strength, and long service life (ACI, 2015). Nonetheless, the transverse thermal expansion of FRP bars is higher than that of concrete. This difference in thermal expansion may cause circumferential tensile cracks in concrete at low temperatures if the confining action of concrete is not sufficient (Zaidi & Masmoudi, 2012). Many

researches on thermal behavior of FRP reinforced concrete elements were investigated taking into account many parameters such as temperature variation, type and diameter of FRP bar, concrete cover thickness, shape of the cross section, and spacing between bars. However, the overlapped FRP bars effect on the thermal behavior of reinforced concrete beams submitted to low temperatures was not investigated in the previous studies (Zaidi & Masmoudi, 2012; Rahman et al., 1995; Masmoudi et al. 2005; Bellakehal et al., 2018). For this reason, a nonlinear numerical investigation using finite element ADINA software is performed to study the thermal behavior of concrete beams reinforced with two vertical overlapped glass FRP (GFRP) bars under low temperature variation of up to -60°C . This study permits to predict transverse thermal strains at the interface of FRP bar/concrete and at the interface of the two FRP bars/concrete and at the external surface of concrete cover varying the ratio of concrete cover thickness to FRP bar diameter for overlapped FRP bars-reinforced concrete beams under low temperatures. Comparisons between transverse thermal strains predicted from the numerical model and those obtained from the analytical model are presented.

2 Nonlinear Numerical Model

A nonlinear numerical model has been established using ADINA software to investigate the prismatic concrete beams reinforced with two overlapped glass FRP (GFRP) bars under low temperature variations of up to -60°C , varying the ratio of concrete cover thickness to FRP bar diameter (c/d_b) from 1 to 3.2. The cross-section of beams had dimensions ($b_o \times h$) of 76×100 ; 100×125 and $100 \text{ mm} \times 150 \text{ mm}$. Five GFRP bars diameters (d_b) have been used 9.5; 12.7; 15.9; 19.1 and 25.4 mm. The concrete cover thickness (c) considered was equal to 20; 25; 30 and 35 mm. Details of GFRP bars-reinforced concrete beams are illustrated in Figure 1. The GFRP bars used had a linear elastic behavior; however, the concrete had a nonlinear behavior. Both materials were supposed to have a perfect bond at the interface level. GFRP bars properties and concrete are described in Table 1 and 2, respectively.

The coefficient of thermal expansion (CTE) of concrete measured using experimental tests was equal to $11.6 \times 10^{-6}/^{\circ}\text{C}$. The average tensile strength (f_{ct}) and compressive strength (f'_c) have been determined according to ASTM standard tests (ASTM, 2002a, 2002b). The Poisson's ratio of concrete (ν_c) has been considered equal to 0.17. The concrete elasticity modulus (E_c) has been evaluated according to CAN/CSA-S806-02 guidelines. The longitudinal CTE of GFRP bars obtained by experimental tests was found to be equal to $\alpha_l = 8 \times 10^{-6}/^{\circ}\text{C}$ while the transverse CTE was found to be equal to $\alpha_t = 33 \times 10^{-6}/^{\circ}\text{C}$. The elasticity modulus (E_t) and Poisson's ratio (ν_{tt}) of GFRP bars in the transverse direction were determined theoretically using the rule of mixture and were found equal to 7.1 GPa and 0.38, respectively. The cross-section of overlapped GFRP bars-reinforced concrete beam was modeled by means of two dimensional plane stress elements because of the constant of the axial deformations. The study has been carried out only for the half of the cross-section of concrete beams since the cross-section is symmetric respect to z-z axis. The temperature variation (ΔT) applied statically on the concrete and the overlapped GFRP bars, was decreased from 0 to -60°C with an increment of -5°C . The meshing of the concrete and the overlapped GFRP bars was established using triangular elements with six nodes, as shown in Figure 1(c). Moreover, the GFRP bars and the concrete materials share the same nodes at the interface.

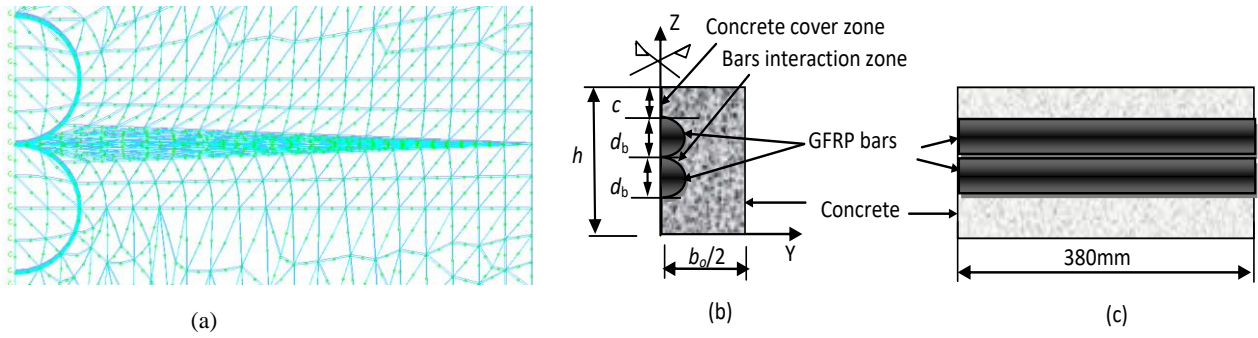


Fig. 1: Detail of reinforced concrete beam: (a) Meshing of the both GFRP bars and concrete through the width $b_o/2$, (b) The half of the modelled cross-section of beam, (c) Concrete beam reinforced with two overlapped GFRP bars

Table 1: Mechanical properties of glass FRP (GFRP) bars

Bar diameter d_b , mm	Ultimate tensile strength f_{fu} , MPa	Longitudinal modulus of elasticity E_l , GPa	Longitudinal Poisson's ratio, ν_l	Ultimate tensile Deformation (%)
9.5	627 ± 22	42 ± 1	0.28 ± 0.02	1.8 ± 0.2
12.7	617 ± 16	42 ± 1	0.28 ± 0.02	1.5 ± 0.2
15.9	535 ± 9	42 ± 1	0.28 ± 0.02	1.4 ± 0.2
19.1	600 ± 15	40 ± 1	0.28 ± 0.02	1.5 ± 0.2
25.4	N/a	N/a	0.28 ± 0.02	N/a

Table 2: Mechanical and physical properties of concrete

Compressive strength f'_{c28} , MPa	Tensile strength f_{ct28} , MPa	Modulus of elasticity E_c , GPa	Coefficient of thermal expansion, α_c ($\times 10^{-6}/^\circ\text{C}$)
40 ± 3	4.1 ± 0.1	28 ± 2	11.6 ± 2.1

3 Linear Analytical Model

Based on research works carried out by Bellakehal et al. (2018) on concrete beam reinforced with two overlapped GFRP bars under high temperature, the following analytical model is developed for overlapped two FRP bars embedded in prismatic concrete element under low temperatures. The radial tensile stresses $\sigma_{\rho 1}$ due to the radial pressure P_1 exerted by FRP bar1 and $\sigma_{\rho 2}$ due to the radial pressure P_2 exerted by FRP bar2, in a concrete element situated at a distance ρ measured from the each FRP bar center, as shown in Figure 2, are given as follows:

$$\sigma_{\rho 1}(\rho) = \frac{P_1}{r_1^2 - 1} \left(1 - \frac{b_1^2}{\rho^2} \right) \quad (1)$$

$$\sigma_{\rho 2}(\rho) = \frac{P_2}{r_2^2 - 1} \left(1 - \frac{b_2^2}{\rho^2} \right) \quad (2)$$

Where, $r_1 = \frac{2c_1 + d_b}{d_b}$; $r_2 = \frac{2c_2 + d_b}{d_b}$; $b_1 = c_1 + a$; $b_2 = c_2 + a$; $a = d_b / 2$; c_1 and c_2 are the concrete cover thickness of the first and the second FRP bars, respectively. The radial pressures P_1 and P_2 exerted by the first and the second FRP bars, respectively, are given by the following expressions:

$$P_1 = \frac{(\alpha_t - \alpha_c)\Delta T}{\frac{1}{E_c} \left(\frac{r_1^2 + 1}{r_1^2 - 1} + \nu_c \right) + \frac{1}{E_t} (1 - \nu_u)} \quad (3)$$

$$P_2 = \frac{(\alpha_t - \alpha_c)\Delta T}{\frac{1}{E_c} \left(\frac{r_2^2 + 1}{r_2^2 - 1} + \nu_c \right) + \frac{1}{E_t} (1 - \nu_u)} \quad (4)$$

Where, E_c is the modulus of elasticity of concrete; ν_c is Poisson's ratio of concrete; α_c is the coefficient of thermal expansion of concrete; E_t is the modulus of elasticity of the FRP bar in the transverse direction; ν_u is Poisson's ratio of the FRP bar in the transverse direction and α_t is the transverse coefficient of thermal expansion of FRP bar.

For FRP bar1 (Figure 2), the maximum radial tensile stress due to the radial pressure P_1 at the interface of FRP bar1/concrete in the concrete cover zone is obtained from Eq.(1) for $\rho = a$:

$$\sigma_{\rho 1max} = -P_1 \quad (5)$$

For FRP bar2 (Figure 2), the maximum radial tensile stress is:

$$\sigma_{\rho 2max} = -P_2 \quad (6)$$

In the bars interaction zone, the radial tensile stress due to radial pressures P_1 and P_2 exerted by the first and the second FRP bars, respectively, in concrete element situated at a distance ρ from the each bar center (Figure 2), is given as follows:

$$\bar{\sigma}_\rho(\rho) = \bar{\sigma}_{\rho 1}(\rho) + \bar{\sigma}_{\rho 2}(\rho) \Leftrightarrow \sigma^2(\rho) = \sigma_{\rho 1}^2 + \sigma_{\rho 2}^2 + 2\sigma_{\rho 1}\sigma_{\rho 2} \cos(2\alpha) \quad (7)$$

From Eq. (1) and (2) in Eq. (7), the radial tensile stress becomes:

$$\sigma_\rho^2(\rho) = \left[\frac{P_1}{r_1^2 - 1} \left(1 - \frac{b_1^2}{\rho^2} \right) \right]^2 + \left[\frac{P_2}{r_2^2 - 1} \left(1 - \frac{b_2^2}{\rho^2} \right) \right]^2 + \frac{2P_1P_2}{(r_1^2 - 1)(r_2^2 - 1)} \left(1 - \frac{b_1^2}{\rho^2} \right) \left(1 - \frac{b_2^2}{\rho^2} \right) \cos(2\alpha) \quad (8)$$

The maximum radial tensile stress due to radial pressures P_1 and P_2 of the first and the second bars, respectively, in the bars interaction zone, where $\rho = a$ and $\alpha = 0^\circ$, is given by:

$$\sigma_{\rho max}(a) = \sigma_{\rho 1}(a) + \sigma_{\rho 2}(a) = -(P_1 + P_2) \quad (9)$$

The first circumferential cracks appear in concrete cover zone, at the interface of FRP bar1/concrete ($\rho = a$), when the maximum radial tensile stress $\sigma_{\rho 1max}$ reaches the concrete tensile strength f_{ct} ($\sigma_{\rho 1max} = -P_1 = f_{ct}$). Thus, the thermal load producing the first cracks, at the FRP bar1/concrete interface, obtained from Eq. (3) and (5) for $\sigma_{\rho 1max} = f_{ct}$, is given by:

$$\Delta T_{cr1} = \frac{f_{ct}}{(\alpha_t - \alpha_c)} \left[\frac{1}{E_c} + \frac{r_1^2 - 1}{r_1^2 + 1} \left(\frac{\nu_c}{E_c} + \frac{1 - \nu_u}{E_t} \right) \right] \quad (10)$$

While, the thermal load producing the first crack, in the concrete of bars interaction zone taking account of the two overlapped bars effect, is obtained from Eq. (9), (4) and (3) when $\sigma_{\rho max} = f_{ct}$, as follows:

$$\Delta T_{cr} = \frac{-f_{ct}}{(\alpha_t - \alpha_c)} \left[\frac{1}{\frac{1}{E_c} \left(\frac{r_1^2 + 1}{r_1^2 - 1} + \nu_c \right) + \frac{1}{E_t} (1 - \nu_{tt})} + \frac{1}{\frac{1}{E_c} \left(\frac{r_2^2 + 1}{r_2^2 - 1} + \nu_c \right) + \frac{1}{E_t} (1 - \nu_{tt})} \right]^{-1} \quad (11)$$

The transverse strain ε_{ct1} in the concrete cover zone, at FRP bar1/concrete interface ($\rho = a$), due to the radial pressure P_1 and the temperature variation ΔT , is given by:

$$\varepsilon_{ct1} = \frac{P_1}{E_c} \left(\frac{r_1^2 + 1}{r_1^2 - 1} + \nu_c \right) + \alpha_c \Delta T \quad (12)$$

Nevertheless, the transverse thermal strain ε_{ct} due to the radial pressures P_1 and P_2 exerted by the first and the second FRP bars (bar1 and2), respectively, at the interface of the two bars/concrete ($\rho = a$), and also the temperature variation ΔT , is given by:

$$\varepsilon_{ct} = \varepsilon_{ct1}(a) + \varepsilon_{ct2}(a) = \frac{P_1}{E_c} \left(\frac{r_1^2 + 1}{r_1^2 - 1} + \nu_c \right) + \frac{P_2}{E_c} \left(\frac{r_2^2 + 1}{r_2^2 - 1} + \nu_c \right) + \alpha_c \Delta T \quad (13)$$

The transverse thermal strain ε_{ct1} in concrete, at the external surface of concrete cover zone ($\rho = b_1$), due to the radial pressure P_1 and the temperature variation ΔT , is given by:

$$\varepsilon_{ct1} = \frac{2P_1}{E_c(r_1^2 - 1)} + \alpha_c \Delta T \quad (14)$$

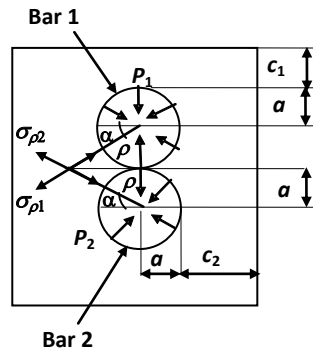


Fig. 2: Analytical model of overlapped FRP bars in concrete under low temperatures.

4 Comparison Between Numerical and Analytical Results

Figures 3 to 8 show comparisons between analytical and numerical curves in terms of transverse thermal strains of concrete at the interface of FRP bar/concrete of the concrete cover zone and at the interface of the two FRP bars/concrete of the bars interaction zone as well as at the external surface of the concrete cover of typical concrete beams reinforced with two overlapped GFRP bars varying c/d_b ratio from 1 to 3.2. It is observed that the transverse thermal strain curve at the bar/concrete interface of the concrete cover zone is linear for temperature variations, in algebraic value, $\Delta T > -30$ °C (Figures 3 and 4). However, for $\Delta T < -30$ °C, in algebraic value, the strain curve becomes parabolic due to the formation of cracks in the concrete surrounding GFRP bars as shown in Figure 9(b). The same remarks can be noted for the thermal transverse strains at the interface of FRP bars/concrete of bars interaction zone except that the change of the slope of strain curves is done in

general at $\Delta T = -10\text{ }^{\circ}\text{C}$ approximately as shown in Figures 5, 6 and 9(a). Furthermore, the transverse thermal strain at the interface of the two GFRP bars/concrete of the bars interaction zone is generally higher, particularly before the failure of the concrete cover compared to that predicted at the interface of FRP bar/concrete of the concrete cover zone. In addition, it is observed that transverse thermal strain curves at the external surface of concrete cover are linear for beams having ratios $c/d_b \geq 2$ (Figure 7), because cracks did not reach the external surface of concrete cover of these beams. However, for ratios $c/d_b < 2$ (Figure 8), the transverse thermal strain curves are linear up to the temperature variation ΔT_{sp} , producing the failure of concrete cover, from which the thermal strain curves become parabolic because of cracks, which reached the external surface of concrete cover as shown in Figure 9(c). In addition, transverse strain curves predicted from the non-linear numerical model are in good agreement with those obtained from the linear analytical model until thermal loads ΔT around $-30\text{ }^{\circ}\text{C}$, $-10\text{ }^{\circ}\text{C}$, $-30\text{ }^{\circ}\text{C}$ measured, respectively, at the interface of FRP bar/concrete of the concrete cover zone, at the interface of the two FRP bars/concrete of the bars interaction zone, and at the external surface of the concrete cover. Beyond these thermal load values, transverse thermal strains predicted from the numerical model are higher than those evaluated by the linear analytical model because of cracks developed within concrete, which are not considered in the analytical model.

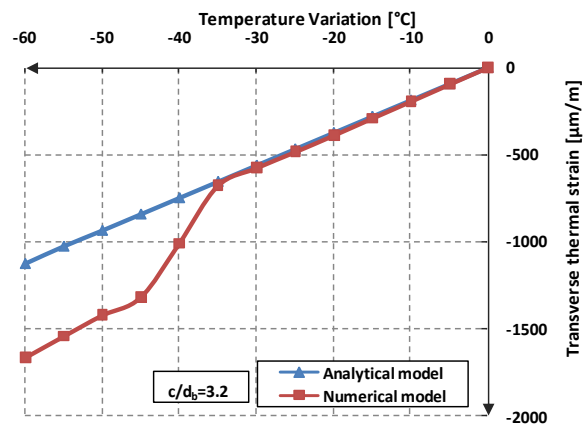


Fig. 3: Transverse thermal strain at FRP bar/concrete interface of concrete cover zone of beam having $c/d_b = 3.2$ - Comparison between analytical and numerical results

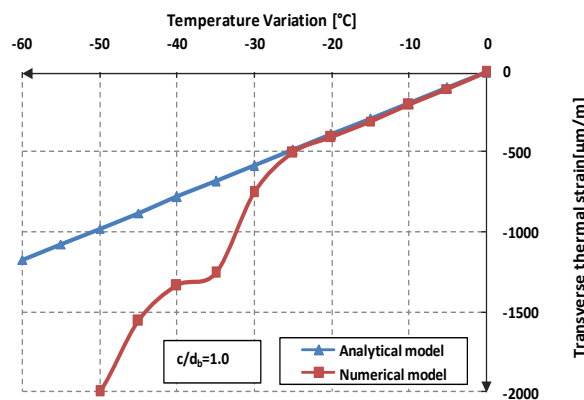


Fig. 4: Transverse thermal strain at FRP bar/concrete interface of concrete cover zone of beam having $c/d_b = 1.0$ - Comparison between analytical and numerical results

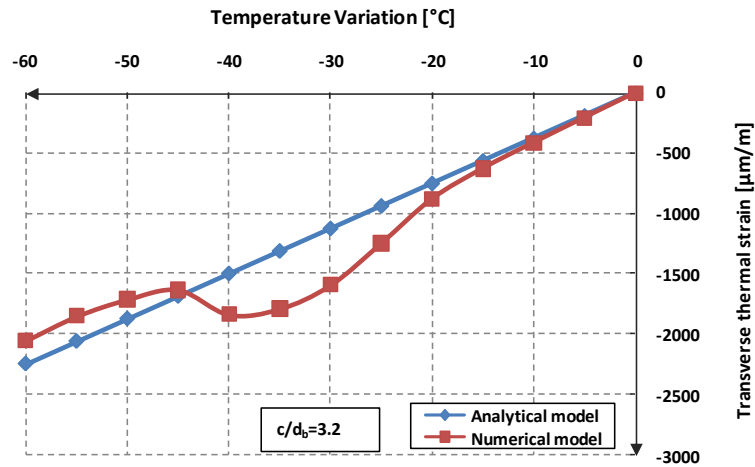


Fig. 5: Transverse thermal strain at two FRP bars/concrete interface of bars interaction zone of beam having $c/d_b = 3.2$ - Comparison between analytical and numerical results

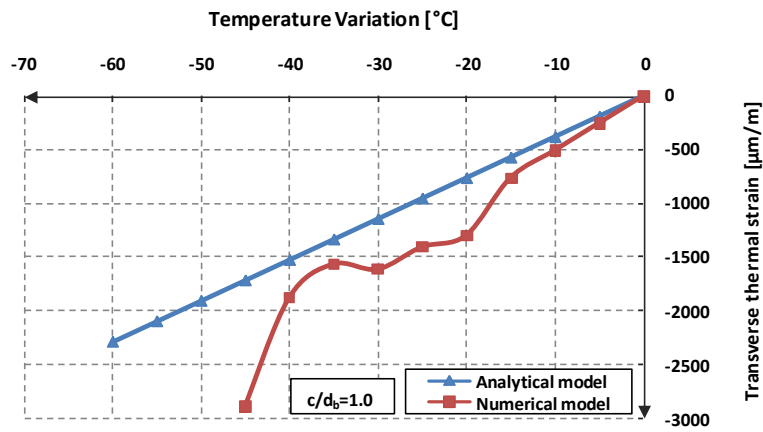


Fig. 6: Transverse thermal strain at two FRP bars/concrete interface of bars interaction zone of beam having $c/d_b = 1.0$ - Comparison between analytical and numerical results

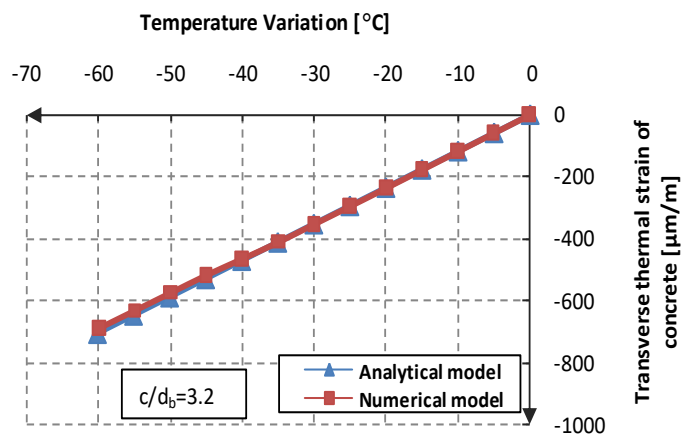


Fig. 7: Transverse thermal strain of concrete at external surface of concrete cover zone of beam having $c/d_b = 3.2$ - Comparison between analytical and numerical results

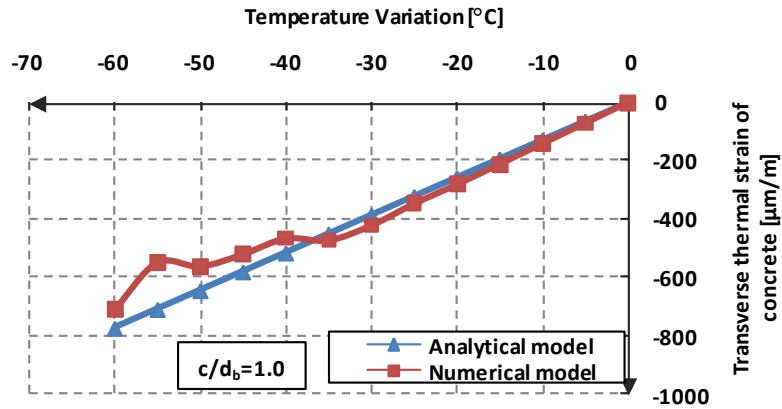


Fig. 8: Transverse thermal strain of concrete at external surface of concrete cover zone of beam having $c/d_b = 1.0$ - Comparison between analytical and numerical results

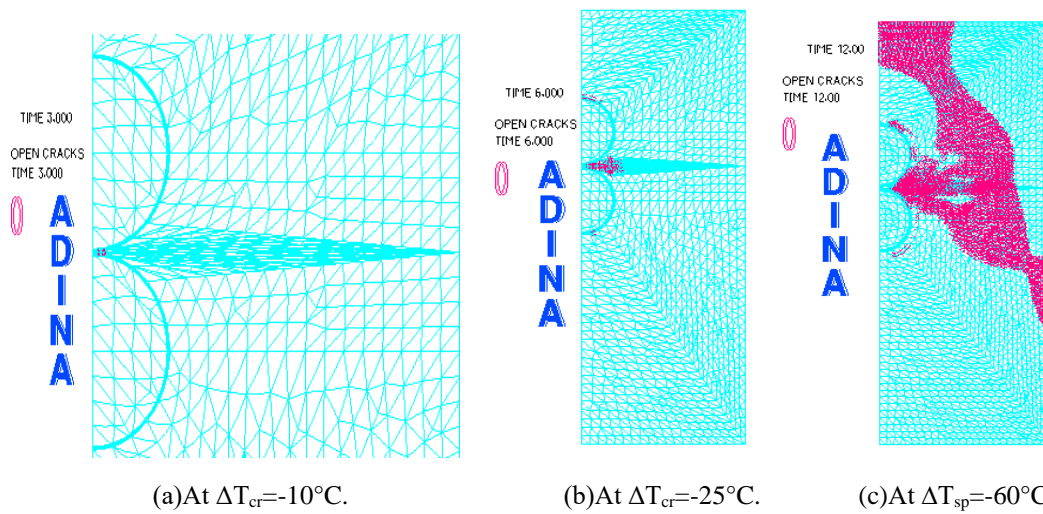


Fig. 9: Cracks development in concrete at FRP bar/concrete interface for concrete cover zone and bars interaction zone (Beam having $c/d_b = 1$): (a) First cracks at bars interaction zone; (b) First cracks at concrete cover zone; (c) Failure of concrete cover

5 Conclusion

Analytical and numerical analysis of low temperature effects on thermal deformations of two glass FRP bars embedded in a prismatic concrete beam, allow to draw the following conclusions:

- From the linear analytical model, GFRP bar diameter and concrete cover thickness variations do not have a great influence on transverse thermal strain which depend mainly on the temperature variation.
- Numerical and analytical results in terms of transverse thermal strains at the FRP bar/concrete interface of concrete cover zone and at the interface of two FRP bars/concrete of bars interaction zone of prismatic beams, are almost similar for $\Delta T > -30$ °C and $\Delta T > -10$ °C, respectively. However, for $\Delta T \leq -30$ °C and $\Delta T \leq -10$ °C, the numerical strains are higher because of circumferential cracks developed in concrete, which are not taken into account in the analytical model.

References

- American Concrete Institute. (2015). Guide for the Design and Construction of Concrete with FRP Bars, ACI 440.1R-15, Farmington Hills, Mich.
- American Society for Testing and Materials. (2002a). Standard test method for splitting tensile strength of cylindrical concrete specimens, In: annual book of ASTM standards, *ASTM C 496-96, USA, 04(2)*: 281–4.
- American Society for Testing and Materials. (2002b). Standard test method for compressive strength of cylindrical concrete specimens, In: Annual book of ASTM standards, *ASTM C 39/C 39M-01, USA, 4(2)*: 21–5.
- Bellakehal, H. et al. (2018). Theoretical Analysis of Thermal Behavior of Overlapped GFRP Bars Embedded in Reinforced Concrete Beams. *Arabian Journal for Science and Engineering, Springer, 43(10)*: 5255–5263. <https://doi.org/10.1007/s13369-018-3086-5>.
- Canadian Standards Association. (2002). Design and construction of building components with fiber–reinforced polymers, CAN/CSA-S806-02, Toronto, Ontario, Canada.
- Masmoudi, R., Zaidi, A. & Gérard, P. (2005). Transverse thermal expansion of FRP bars embedded in concrete, *Journal of composites for construction, 9(5)*: 377-387. [https://doi.org/10.1061/\(ASCE\)1090-0268\(2005\)9:5\(377\)](https://doi.org/10.1061/(ASCE)1090-0268(2005)9:5(377))
- Rahman, H.A., Kingsley, C. Y. & Taylor, D.A. (1995). Thermal stress in FRP reinforced concrete, Proceedings of Annual Conference of the Canadian Society for Civil Engineering, Ottawa, Canada, 605-614.
- Zaidi, A. & Masmoudi, R. (2012). Numerical Analysis of Thermal Behavior of Concrete Cover around FRP-Bars in Cold Region, *Arabian Journal for Science and Engineering, Springer, 37(2)*: 489-504. <https://doi.org/10.1007/s13369-012-0173-x>.

Cite as: Zaidi A., Bellakehal H., Masmoudi R., Terbagou O. & Nia N., “Theoretical Simulation of Thermal Deformations in Concrete Beams Reinforced with Two Overlapped FRP Bars in Cold Regions”, *The 2nd International Conference on Civil Infrastructure and Construction (CIC 2023)*, Doha, Qatar, 5-8 February 2023, DOI: <https://doi.org/10.29117/cic.2023.0061>